

# Large and High Power Cylindrical Batteries – Analysis of the Battery Packs Temperature Distributions Using COMSOL Multiphysics® and MATLAB® Simulation Softwares

O. Capron<sup>\*1</sup>, A. Samba<sup>1,2</sup>, N. Omar<sup>1</sup>, H. Gualous<sup>2</sup>, P. Van den Bossche<sup>1</sup>, J. Van Mierlo<sup>1</sup>

<sup>1</sup>MOBI-Mobility, Logistics and Automotive Technology Research Centre, VUB – Vrije Universiteit Brussel, Brussels, BELGIUM

<sup>2</sup>Laboratoire LUSAC, Université de Caen Basse Normandie, Cherbourg-Octeville, FRANCE

\*Corresponding author: Pleinlaan, 2 1050 Elsene BELGIUM, [ocapron@vub.ac.be](mailto:ocapron@vub.ac.be)

**Abstract:** A good cooling inside a battery pack is important to avoid safety issues and avoid the development of too large internal temperature gradients. The temperature distributions inside two packs (in-line and staggered) made of large cylindrical lithium iron phosphate cells (of 18 Ah nominal capacity) are analysed in this paper during a 90 A constant discharge current. The analysis of the battery packs temperature distributions is based on the results obtained with a two-dimensional modelling approach. For both packs, the simulations results indicate that a better cooling of the cells located at the rear of the packs occurs with the increase of the air inlet velocity. In these packs, the regions inside the cells show the highest temperature values and a faster temperature increase in time compared to the cells surface regions.

**Keywords:** cooling, in-line pack, staggered pack, temperature distribution, two-dimensional.

## 1. Introduction

For lithium-ion batteries the best operating temperatures are in the range between 25°C and 40°C [1]. To avoid the occurrence of an excessive temperature rise [2] leading to the degradation in their lifetime or even worse to the thermal runaway phenomenon, local temperature of lithium-ion batteries should be carefully monitored. For a battery pack, the operating temperature and the uniformity of the temperature distribution inside the pack are two important factors [3]. Inside the pack, the non-uniformity of the temperature can even lead to the non-uniformity of the performances of the individual cells [4].

For these reasons, many researches have been done on the modelling of battery packs from the thermal point of view. Among others, in

[5] a three-dimensional electro-thermal study of battery packs (in-line and staggered) made of small cylindrical 26650 cells (0.026 m diameter) has been conducted. In [6] a two dimensional computational fluid dynamics model of an in-line battery pack made of small 26650 cells has been developed. However, no two-dimensional study has been conducted so far regarding the thermal behaviour of battery packs made of large cylindrical cells.

In this paper, the analysis of the temperature distribution for two battery packs configurations (in-line and staggered) is achieved using a two-dimensional modelling approach. Both packs are made of large (0.06 m diameter) cylindrical lithium iron phosphate cells of 18 Ah nominal capacity. Compared to the use of three-dimensional packs models, this two-dimensional modelling approach presented in this paper allows to reduce the computational time. Based on this modelling approach, the effects of the air inlet velocity and the distance between two consecutive cells, on the temperature distribution inside both in-line and staggered battery packs were highlighted.

## 2. Modelling approach

The modelling of lithium-ion battery cells involves different length scale physics.

To investigate the thermal behaviour of both in-line and staggered battery packs made of large lithium-ion cylindrical cells, a coupling between the lithium-ion battery physics and the heat transfer (closed packs) or conjugate heat transfer (open packs) has been implemented in COMSOL Multiphysics®. For the simulations, all the cells of both in-line and staggered battery packs were discharged with a 90A (5C) constant current.

In the context of a previous study, the thermal conductivity of a large individual cylindrical cell in the longitudinal direction was observed to be much greater compared to the thermal conductivity value in the radial direction of the cell. Therefore, for a single cell the temperature gradients observed in the longitudinal direction are significantly lower in value compared to the ones in the radial direction. Considering the smaller temperature difference in the longitudinal direction compared to the radial direction of each single cell at the end of the 90A (5C) constant current discharge, a reduced two-dimensional packs thermal study was achieved in this paper.

The post-processing of the simulations results obtained with COMSOL<sup>®</sup> was achieved within MATLAB<sup>®</sup> thanks to the COMSOL LiveLink<sup>™</sup> for MATLAB<sup>®</sup>. Combining COMSOL<sup>®</sup> with MATLAB<sup>®</sup> allowed for writing several MATLAB<sup>®</sup> scripts that were used to conduct an efficient and a flexible analysis of the simulations results.

### 3. Use of COMSOL Multiphysics<sup>®</sup>

#### 3.1 Model geometries

Both in-line and staggered pack configurations are studied in this paper with a two-dimensional approach. Two types of packs can be defined based on the distance between two consecutive cells located on the same row inside the pack. Table 1 summarizes the geometrical dimensions used for the implementation of these packs in COMSOL Multiphysics<sup>®</sup>.

**Table 1** Packs geometrical parameters

Parameters	Pack type 1	Pack type 2
Cells inter-distance, (center to center), [m]	0.063	0.08
Pack width, [m]		
<i>In-line</i>	0.16	
<i>Staggered</i>	0.24	
Pack length, [m]		
<i>In-line</i>	0.292	0.36
<i>Staggered</i>	0.229	0.28

Distance from bottom or top of the cells to the side of the pack, [m]	0.01
Distance from the left or right of the cells to the side of the pack, [m]	0.01
Distance between two rows of cells, [m]	0.02

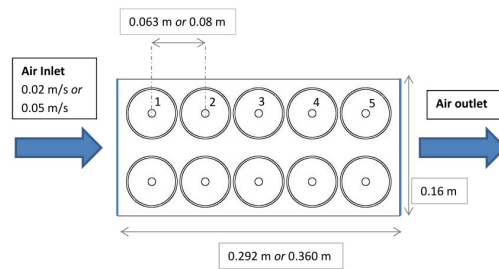


**Figure 1** Schematic of the in-line pack

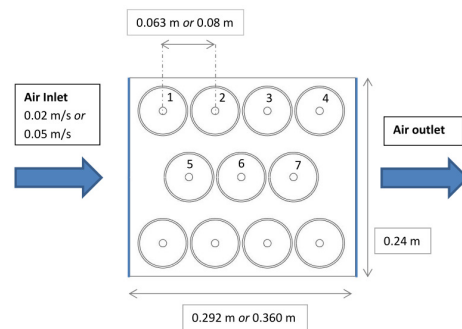


**Figure 2** Schematic of the staggered pack

#### 3.2 Coolant fluid and material properties

Table 2 summarises the coolant fluid and the material thermal properties used to model the two pack configurations.

**Table 2** Fluid and material properties

Material	Properties	Value
Air (Gas)	$\rho$ , [kg/m <sup>3</sup> ]	Defined by piecewise functions dependent on the temperature
	$C_p$ , [J/kg.K]	
	$k$ , [W/m.K]	
Steel AISI 4340	$\rho$ , [kg/m <sup>3</sup> ]	7850
	$C_p$ , [J/kg.K]	475
	$k$ , [W/m.K]	44.5

<b>Battery active material</b>	$\rho$ , [kg/m <sup>3</sup> ]	3345.5
	$C_p$ , [J/kg.K]	1034.2
	$k$ , [W/m.K]	0.33434

### 3.3 Physics

Table 3 summarizes the physics used for the modelling of the packs.

Since both in-line and staggered pack configurations have a symmetry axis, symmetry conditions for the temperature and the air velocity were also added to the models.

The initial pack temperature for the simulations of both (open or closed) in-line and staggered battery packs is equal to 25°C.

For the open in-line and staggered pack configurations, an air inlet velocity of 0.02 m/s or 0.05 m/s was applied initially to the packs as shown in Figures 1 and 2.

**Table 3** Summary of the physics used

	<b>Closed pack</b>	<b>Open pack</b>
<b>Physics</b>	<i>Heat Transfer in Solids</i>	<i>Conjugate Heat Transfer</i>

### 3.4 Mesh study

Once the physics were assigned, we applied a user-controlled mesh made of a free triangular meshing process (maximum element size of 0.000402 and minimum element size of 1.8E-4) over the different battery pack geometries. The same mesh was used for all the packs geometries, to compare the results. This mesh guarantees a reasonable computational time for the results obtained.

## 4. Results and Discussion

### 4.1 Closed packs – Temperature distribution

To assess the importance of cooling strategies for battery packs, Figures 3 and 4 show the temperature distributions at the end of the simulation with a 90A constant discharge current (610s) obtained inside a closed pack (no inlet, no outlet nor air velocity). Figures 3 and 4 represent the in-line and the staggered pack configurations with a distance between two

consecutive cells on the same row equal to 0.063 m (Pack type 1).

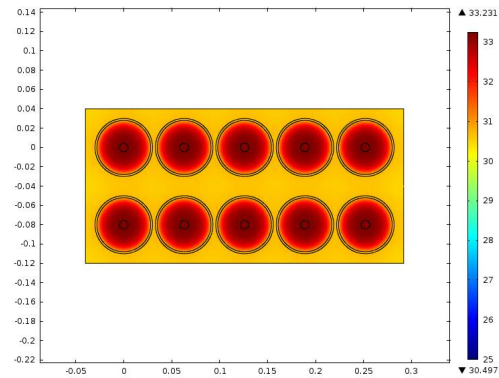


**Figure 3** Temperature distribution in a closed in-line pack (d=0.063 m) at t=610s

Figures 3 and 4 indicate that the temperature inside the cells at the end of the discharge is in the range between 32°C and 33°C, while the temperature of the air around is about 31°C.

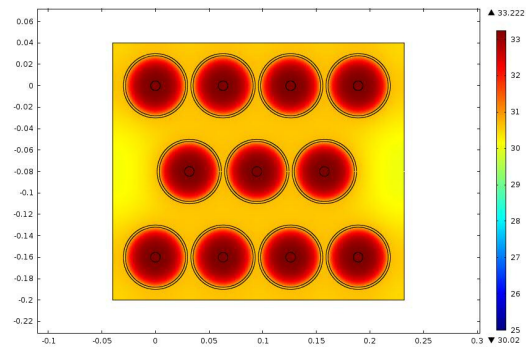


**Figure 4** Temperature distribution in a closed staggered pack (d=0.063 m) at t=610s

Because of the small temperature difference between the cells internal temperatures and the air temperature around the cells, Figures 3 and 4 emphasize the need for cooling strategies of these packs.

### 4.2 Open packs - Non-zero coolant fluid velocities

To see the influence of a coolant fluid on the packs temperature distributions, the packs are made now open.

### Air velocity of 0.02 m/s

As indicated in Figures 1 and 2, a 0.02 m/s air inlet velocity is assigned to the left-hand side vertical boundary of both in-line and staggered packs.

Figures 5 and 6 present the results of the air velocity field inside both packs.

For both in-line and staggered packs, the maximum air velocities (0.1457 m/s and 0.1172 m/s) are observed in between each row of cells. Indeed, the air does not encounter any obstacles in these regions.

Conversely, the lowest velocities (between 0 and 0.02 m/s) are observed in the less accessible regions (i.e. in between two consecutive cells on a same row).

For these velocity fields, Figures 7 and 8 present the temperature distributions obtained inside the packs at the end of the simulation time (610s).

In Figures 7 and 8, the regions that were observed with the highest air velocities show now the lowest temperatures.

However the regions at the rear of the packs and in between the cells on a same row, still present great temperature values (greater than 30°C) compared to the initial 25°C temperature.

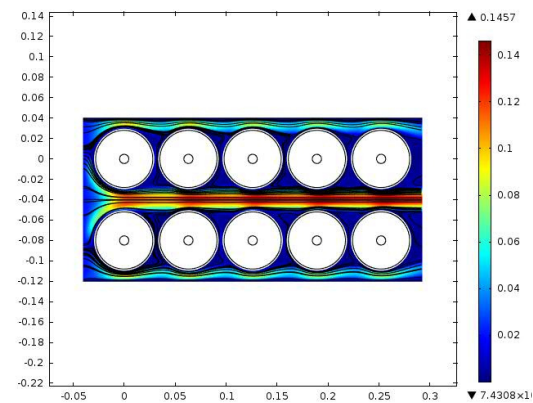


**Figure 5** Velocity field in an in-line pack ( $d=0.063$  m) for a 0.02 m/s air inlet velocity ( $t=610$ s)

Figures 7 and 8 also show that the 25°C temperature region at the front of the packs does not reach (at the end of the simulation time) the rear of the packs.

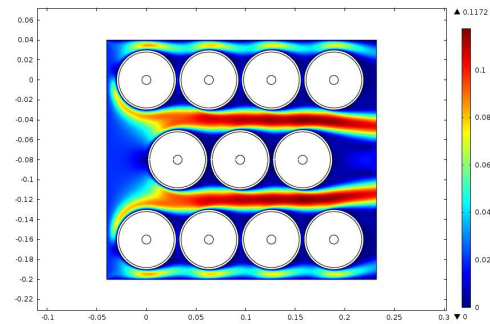


**Figure 6** Velocity field in a staggered pack ( $d=0.063$  m) for a 0.02 m/s air inlet velocity ( $t=610$ s)

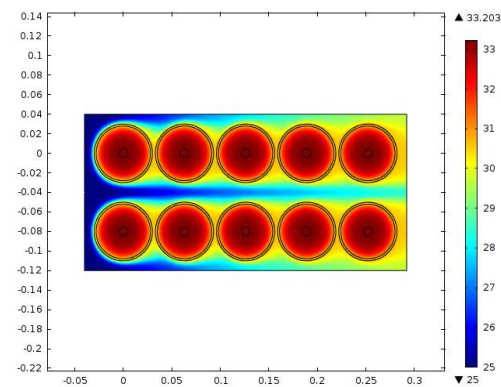


**Figure 7** Temperature distribution in an in-line pack ( $d=0.063$  m) for a 0.02 m/s air inlet velocity ( $t=610$ s)

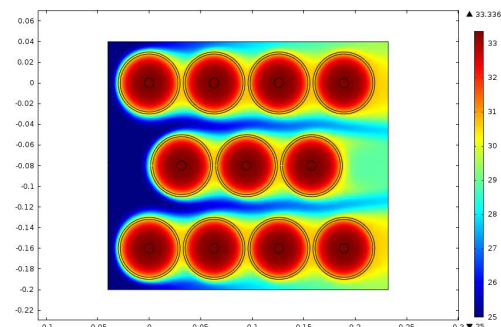


**Figure 8** Temperature distribution in a staggered pack ( $d=0.063$  m) for a 0.02 m/s air inlet velocity ( $t=610$ s)

To enable this 25°C temperature region to develop towards the rear of the packs, higher air inlet velocities are needed.

### Air velocity of 0.05 m/s

Figures 9 and 10 illustrate the packs temperature distributions obtained for both in-line and staggered pack configurations with a 0.05 m/s air inlet velocity. With the increase of the air inlet velocity, the top and the bottom of the last cells of the rows reach lower temperatures (between 25 °C and 29 °C). The 25 °C temperature region is now also observed at the rear of the packs, which highlights an improved cooling achieved for the last cells of the top and bottom rows.

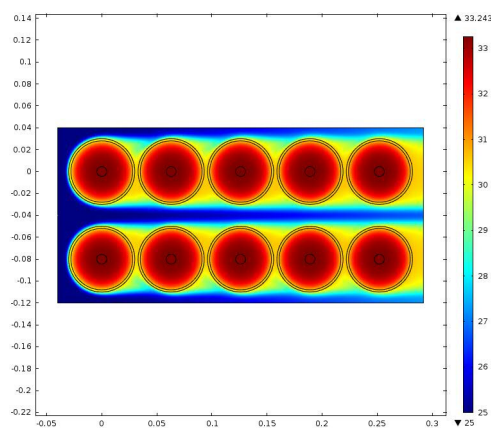


**Figure 9** Temperature distribution in an in-line pack (d=0.063 m) for a 0.05 m/s air inlet velocity (t=610s)

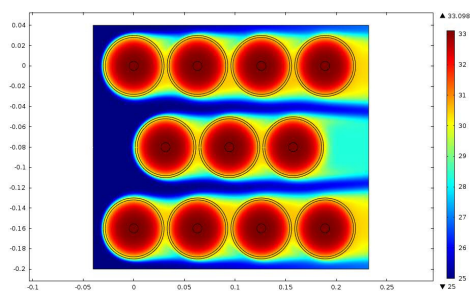


**Figure 10** Temperature distribution in a staggered pack (d=0.063 m) for a 0.05 m/s air inlet velocity (t=610s)

### **4.3 Open packs - Distance between the cells**

For a 0.05 m/s air inlet velocity, Figures 11 and 12 present the air velocity field inside both packs for a distance between two consecutive cells on a row equal to 0.08 m.

As in Figures 5 and 6, the air reaches higher velocities in the regions between two rows of cells. In Figures 11 and 12 the flow of air in between two consecutive cells on a same row is now improved compared to Figures 5 and 6.

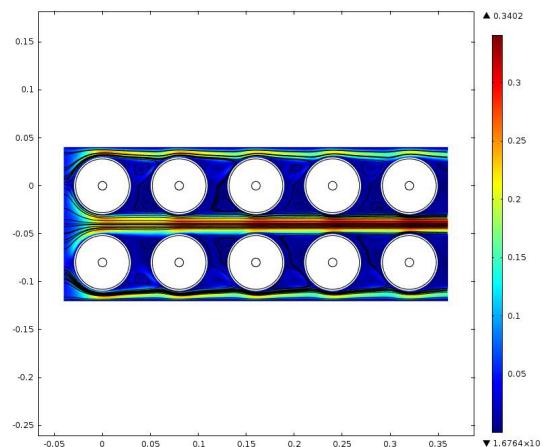


**Figure 11** Velocity field in an in-line pack (d=0.08 m) for a 0.05 m/s air inlet velocity (t=610s)

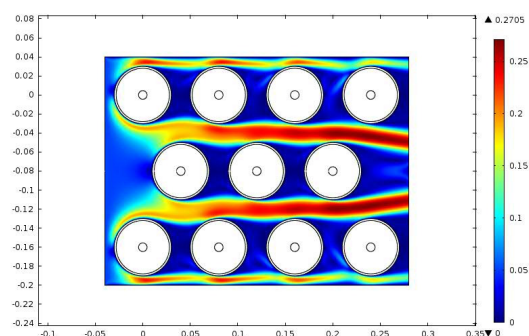


**Figure 12** Velocity field in a staggered pack (d=0.08 m) for a 0.05 m/s air inlet velocity (t=610s)

Figures 13 and 14 present the temperature distributions at the end of the simulation time (610s) obtained inside both packs for a distance between two consecutive cells equal to 0.08 m.

Since the flow of air is now improved in between each consecutive cell on a same row, these regions reach now slightly lower temperatures (compared to Figures 7 and 8) and an improved cooling of these regions is achieved.

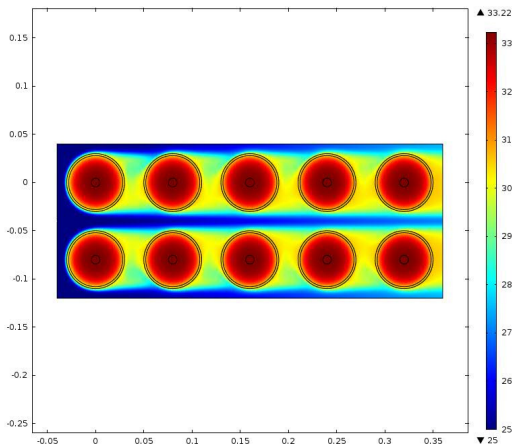


**Figure 13** Temperature distribution in an in-line pack ( $d=0.08$  m) for a 0.05 m/s air inlet velocity ( $t=610$ s)

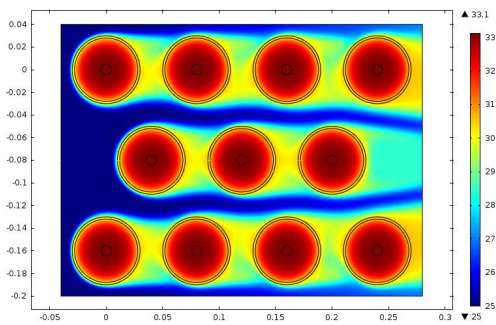


**Figure 14** Temperature distribution in a staggered pack ( $d=0.08$  m) for a 0.05 m/s air inlet velocity ( $t=610$ s)

#### 4.4 Cells temperature evolutions in time

Figure 15 illustrates the cells temperature evolutions in time for the in-line pack configuration. In this battery pack, the air inlet velocity is equal to 0.05 m/s and the distance between each consecutive cell on the same row is set to 0.063 m.

For the surface temperature of the cells, the curves obtained represent the temperatures on the top row of the pack at the front of each cell.

In Figure 15 the cells internal temperature curves clearly show a steeper slope compared to the cells outer surface temperature curves. The increase in the temperature over time is much more significant for the cells internal regions compared to the surface (or external) regions.

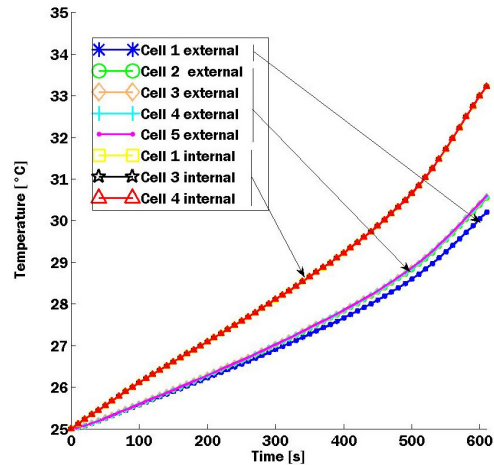


**Figure 15** Cells temperature evolutions in time inside an in-line pack ( $d=0.063$  m) with a 0.05 m/s air inlet velocity

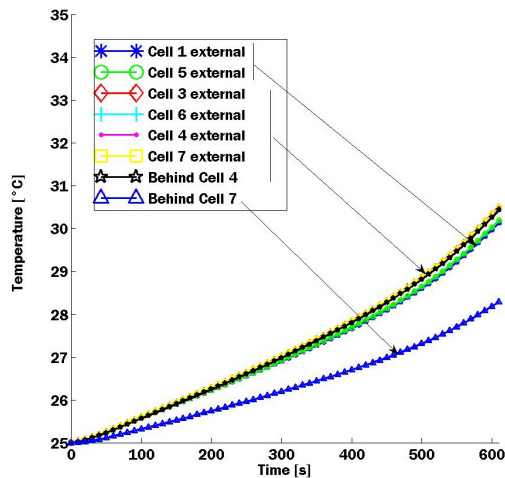
The first cell at the front of the pack on the top row shows slightly lower surface temperature values compared to the other cells on the same row. With the symmetry property of the pack, the results obtained for the cells on the top row are also valid for the cells on the bottom row.

Figure 16 illustrates the cells temperature evolutions in time inside a staggered pack. The air inlet velocity applied to the pack is equal to 0.05 m/s and the distance between two consecutive cells is equal to 0.063 m. These curves represent the surface temperatures on the top and the middle rows of the pack at the front of the each cell.

In Figure 16 the first cells on the top and the middle rows show slightly lower surface temperatures compared to the others cells.

The temperature of the region behind the last cell of the top row shows a faster increase in time compared to the region behind the last cell of the middle row.

At the end of the simulation time, the regions behind the last cell of the top row will reach a temperature between 30 and 31°C, while a temperature around 28°C will be observed behind the last cell of the middle row.



**Figure 16** Cells temperature evolutions in time inside a staggered pack ( $d=0.063$  m) with a  $0.05$  m/s air inlet velocity

The thermal behaviour of the cells on the bottom row can be derived by symmetry from the results obtained for the cells on the top row.

The evolutions in time of the internal temperature of the cells inside the staggered pack are similar to the internal temperature evolutions of the cells inside the in-line pack in Figure 15.

## 5. Conclusions

In this paper, the thermal analysis of two battery packs configurations (in-line and staggered) made of large cylindrical lithium iron phosphate battery cells was achieved with the COMSOL Multiphysics® (version 4.3) simulation software. Considering the smaller temperature difference observed for each individual cell in the longitudinal compared to the radial direction, this study was conducted in two-dimensions. LiveLink™ for Matlab® was used to access to the data generated from the simulations and especially for the post-processing of the temperature time evolutions curves of the cells inside the packs.

From the packs temperature distributions results, an improved cooling of the cells at the rear of the battery packs is achieved with an increase in the air inlet velocity value. The staggered pack configuration allows for an

improved cooling of the region behind the last cell of the middle row.

An increase in the distance between each consecutive cell on a same row allows the air to flow in between the cells. However this does not allow for a significant reduction in the external nor in the surface temperatures of the cells in these areas.

Inside both in-line and staggered packs, the first cell on each row shows a slightly lower surface temperature increase over time compared to the other cells on the same row.

In both in-line and staggered packs, the cells internal temperature increase over time is much more significant compared to the increase of the cells surface temperature. At the end of the simulations, the greatest temperature values were always observed for the regions inside the cells.

## 6. References

1. A.A. Pesaran, Battery thermal models for hybrid vehicle simulations, *Journal of Power Sources*, vol. **110**, pp. 377-382 (2002)
2. R. Sabbah, R. Kizilel, J.R Selman, Active (air cooled) vs. passive (phase change material) thermal management of high power lithium-ion packs: Limitation of temperature rise and uniformity of temperature distribution, *Journal of Power Sources*, vol. **182**, pp. 630-638 (2008)
3. H. Fathabadi, High thermal performance lithium-ion battery pack including hybrid active-passive thermal management system for using in hybrid/electric vehicles, *Energy*, **Article in Press**, pp. 1-10 (2014)
4. L. Lu, X. Han, J. Li, J. Hua, M. Ouyang, A review on the key issues for lithium-ion battery management in electric vehicles, *Journal of Power Sources*, vol. **226**, pp. 272-288 (2013)
5. Y. Ma, H. Teng, M. Thelliez, Electro-Thermal Modeling of a Lithium-ion Battery System, *SAE Int. J. Engines*, vol. **3**, pp. 306-317 (2010)
6. F. He, X. Li, L. Ma Combined experimental and numerical study of thermal management of battery module consisting of multiple Li-ion cells, *International Journal of Heat and Mass Transfer*, vol. **72**, pp. 622-629 (2014)